ACS Macro Letters

Letter

pubs.acs.org/macroletters

Reproducible Access to Tunable Morphologies via the Self-Assembly of an Amphiphilic Diblock Copolymer in Water

Nghia P. Truong,[†] John F. Quinn,[†] Marion V. Dussert,[†] Nikolle B. T. Sousa,[†] Michael R. Whittaker,*[,†] and Thomas P. Davis*[,†,‡]

[†]ARC Centre of Excellence in Convergent Bio-Nano Science and Technology, Monash Institute of Pharmaceutical Sciences, Monash University, Parkville, Melbourne, Victoria 3052, Australia

[‡]Department of Chemistry, University of Warwick, Coventry CV4 7AL, United Kingdom

Supporting Information

ABSTRACT: We report on the preparation of positively charged crew-cut nanoaggregates in water with various nonspherical (i.e., worm, flower, and large compound) and spherical (i.e., vesicle and sphere) morphologies by the self-assembly of a single diblock copolymer in water. Our facile procedure for preparing positively charged nanoparticles, when combined with the techniques for obtaining negatively charged and neutral nanoaggregates already established by Eisenberg et al., provides a versatile toolbox for the reproducible production of uniformly nanostructured particles with control over both morphology and surface chemistry. Such nanoparticles offer opportunities for the fundamental study of nanobio interactions and may open the door to novel drug and gene delivery applications.

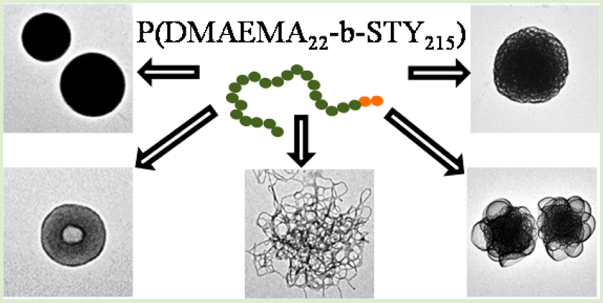

Nanoparticle morphology has been identified as a crucial factor which significantly impacts pharmacokinetics and intracellular trafficking of nanoparticles.[1,2] Preliminary studies into nanoscale drug delivery vehicles have shown that nonspherical morphologies can be useful in tuning circulation time, biodistribution, cellular uptake, and overall efficacy of the delivery system.[3] For example, worm-like nanoparticles (WLN) evade clearance by the immune system and achieve prolonged circulation time, which is a special feature similar to that of certain rod-shaped bacteria, viruses, and fungi found in nature.[4−8] WLN also have the ability to accumulate in tumors to a very high concentration (i.e., up to 30 wt % of the injected dose) and achieve higher antitumor efficacy when compared to spheres (SPH) and vesicles (VES).[9−11] In addition, nanoaggregates with rare morphologies such as large compound vesicles (LCV) and flower-like vesicles (FLV) are rapidly taken up by cells and able to escape endolysosomal cellular transport compartments.[12−14] The unique properties exhibited by nonspherical morphologies make them potentially useful for the design of next-generation nanocarriers for drug and gene therapies.

Notwithstanding the potential benefits outlined above, the structure−property relationship of nanobio interactions occurring between nonspherical nanoparticles and biological systems is still not wholly clear.[15,16] For instance, the effect of nanoaggregate morphology alone on the circulation time, biodistribution, cellular uptake, and toxicity has not been unambiguously demonstrated due to the lack of reproducible synthetic strategies for producing uniformly nonspherical (i.e., WLN, LCV, FLV) and spherical (i.e., SPH, VES) morphologies from the same material (i.e., the same polymer or inorganic matrix).[3] Hence, strategies that can reproducibly yield biocompatible nanoparticles in a variety of different and tunable morphologies from the same material are urgently needed.[17] Such nanoaggregates will enable the thorough characterization of the interactions occurring between biocompatible nanoparticles of varying shape and living cells which, in turn, will guide the development of highly efficacious nanocarriers for drug and gene therapies.[3,17]

Block copolymer (BCP) self-assembly is a versatile method for the production of a wide range of morphologies, including SPH, WLN, VES, and many other complex nanostructures from the same material (i.e., the same polymer).[18,19] Crew-cut nanoaggregates with different morphologies are prepared by first dissolving a highly asymmetric amphiphilic BCP in a common solvent and then adding water to the solution to induce self-assembly or aggregation of the copolymer segments.[20] By varying the self-assembly conditions (e.g., organic solvent used, polymer concentration, water addition rate, etc.), various morphologies can be obtained from the same polymer.[21] In the last two decades, asymmetric amphiphilic BCPs, such as poly(styrene-*b*-acrylic acid) and poly(styrene-*b*-ethylene oxide), have been extensively used for the study of self-assembly in water.[22,23] However, the use of a hydrophobic, glassy polymer (e.g., polystyrene, PSTY) copolymerized with a hydrophilic, positively charged polymer at physiological pH

Received: February 11, 2015
Accepted: March 17, 2015
Published: March 19, 2015

ACS Publications © 2015 American Chemical Society

DOI: 10.1021/acsmacrolett.5b00111
ACS Macro Lett. 2015, 4, 381−386

Scheme 1. Synthesis of Macro-CTA and Diblock Copolymer by RAFT Polymerizations

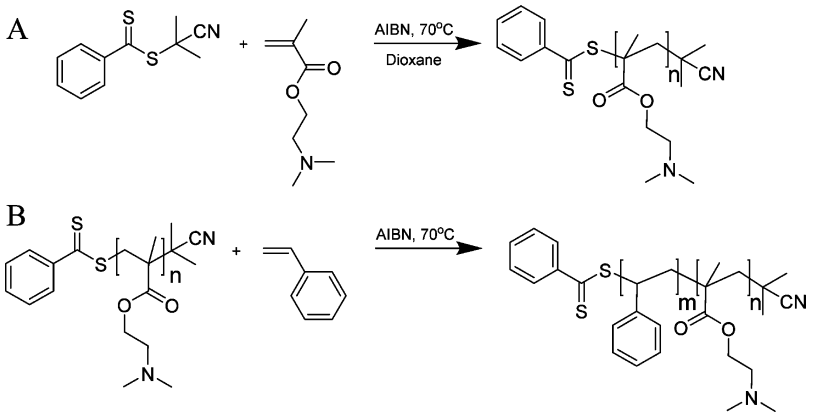

Table 1. Molecular Weight Distribution and ^{1}H NMR Data for P(DMAEMA-b-STY) Copolymers (B1 and B2) Prepared by RAFT Polymerizations of Styrene at 70 °C for 16 h Using AIBN as an Initiator

		SEC[a]		^{1}H NMR			
polymer	[styrene]/[macro-CTA]/[I]	M_n (g/mol)	PDI	conv.[b] (%)	$M_{n,theory}$[c] (g/mol)	repeating unit[d] (n)	$M_{n,NMR}$[e] (g/mol)
B1: P(DMAEMA$_{22}$-*b*-STY$_{215}$)	7700:7:1	31800	1.14	23	29032	215	26035
B2: P(DMAEMA$_{20}$-*b*-STY$_{210}$)	7000:7:1	31600	1.14	24	27704	210	25201

[a]SEC data measured in DMAc + 0.03 wt % of LiBr solution and using PSTY standards for calibration. [b]Conversion of styrene was calculated by the integral area of a peak at 5.7 ppm ($I_{5.7}$) and peaks in the range 6.3−7.5 ($I_{6.3-7.5}$) using the following equation: conv. = $100 \times 5 \times I_{5.7}/I_{6.3-7.5}$. [c]$M_{n,theory}$ was calculated using the following equation: $M_{n,theory}$ = conv. × [STY]/[macro-CTA] × 104 + $M_{n,theory\ of\ macro\text{-}CTA}$. [d]Number of repeating units of styrene was calculated by the integral area of peaks in the range 6.3−7.2 ppm ($I_{6.3}-I_{7.2}$) and a peak at 4.0 ($I_{4.0}$) using the following equation: Repeating units of styrene (n) = $[(I_{4.0}/I_{7.8})/5] \times n_{DMAEMA}$. [e]$M_{n,NMR}$ was calculated using the following equation: $M_{n,NMR} = n \times 104 + M_{n,NMR\ of\ macro\text{-}CTA}$.

(e.g., poly(2-dimethylaminoethyl methacrylate), P(DMAEMA)) for the production of biocompatible nanoaggregates with various morphologies remains an unmet goal.[24]

The aim of this work was to reproducibly prepare positively charged crew-cut nanoaggregates in water with a variety of different yet tunable morphologies (including SPH, LCV, WLN, VES, and FLV) from the same BCP. This was achieved by manipulating the self-assembly of P(DMAEMA$_{22}$-*b*-STY$_{215}$), a highly asymmetric BCP, in water. Well-defined P(DMAEMA$_{22}$-*b*-STY$_{215}$) diblock copolymer was first synthesized by reversible addition−fragmentation chain transfer (RAFT) polymerization. Thereafter, the self-assembly conditions (including organic solvent, copolymer concentration, and water addition rate) were studied and applied to produce nanoparticles with the targeted morphologies. The nanoparticle stability, method reproducibility, and ability to fluorescently label the nanoparticles were also investigated in-depth.

Initially, P(DMAEMA) macromolecular chain transfer agent (macro-CTA) was synthesized by RAFT-mediated solution polymerization at 70 °C for 8.5 h using 2-cyanoprop-2-yl benzodithioate (CBD) as the chain transfer agent, 1,4-dioxane as the solvent, and azobis(isobutyronitrile) (AIBN) as the initiator (see details of synthesis procedures in Scheme 1 and Supporting Information). P(DMAEMA) was chosen as the hydrophilic polymer for this work due to its positive charges at physiological pH (pK_a of P(DMAEMA) is about 7.8) and its biocompatible properties, which are suitable for drug and gene delivery applications.[25−27] The polymerization reaction was repeated twice to study the reproducibility of both polymer synthesis and the self-assembly process. The polymerization conditions were similar to previous reports, except that the temperature was decreased from 90 to 70 °C to reduce side reactions that are known to occur at high polymerization temperature.[28,29] The polymerization was stopped at a conversion of around 60% to further minimize the formation of terminated polymer chains by bimolecular radical coupling at low monomer concentration.[30,31] The molecular weight distribution (MWD) shown in Figure S1 is symmetric and unimodal, confirming the theoretically low number of terminated polymer chains. Further, the very low polydispersity indices (i.e., PDI < 1.1) and the good agreement between M_n determined by SEC, theory, and ^{1}H NMR (see Table S1) indicate the "controlled" characteristics expected under RAFT mechanism and suggest high chain end fidelity for the macro-CTA. In addition, a degree of polymerization (DP) of around 20 (calculated by ^{1}H NMR, see Figure S2) was successfully targeted because this chain length of P(DMAEMA) was in the range of hydrophilic polymer lengths that facilitated the formation of various morphologies and has been found to have little to no toxicity to cells.[32−34] In short, a well-defined macro-CTA suitable for drug and gene delivery applications was reproducibly synthesized by appropriate selection of the monomer, stoichiometry, and polymerization conditions.

The well-defined P(DMAEMA) prepared was subsequently chain extended with styrene by RAFT-mediated polymerization at 70 °C in bulk for 16 h using AIBN as an initiator (see Scheme 1 and Table 1). PSTY was selected as the hydrophobic component to form the nanoparticle cores because the self-assembly of PSTY diblock polymers (e.g., poly(styrene-*b*-acrylic acid) and poly(styrene-*b*-ethylene oxide)) has been intensively studied over the last 20 years by Eisenberg's group.[18,20,24] These previous studies provide excellent guidelines for the selection of the self-assembly conditions for P(DMAEMA-*b*-STY) as applied herein. Further, nanoparticles with stable

DOI: 10.1021/acsmacrolett.5b00111
ACS Macro Lett. 2015, 4, 381−386

styrenic cores have been successfully used for in vitro and in vivo drug delivery applications, which suggests that nanoaggregates produced from P(DMAEMA-*b*-STY) may also be useful in this field.[35−37] The DP of styrene was targeted to be around 200 (i.e., 10× higher than that of DMAEMA) by keeping the conversion of the polymerization at approximately 23% (see Table 1). This chain length of PSTY and the high molar ratio of hydrophobic to hydrophilic units were judiciously selected, based on previous work, to target the expected morphologies (i.e., SPH, LCV, WLN, VES, and FLV).[38,39] By keeping the conversion low, well-defined P(DMAEMA-*b*-STY) with M_n of 3.2 × 10^4 g mol^{-1} was successfully synthesized and characterized (see Figure 1). A

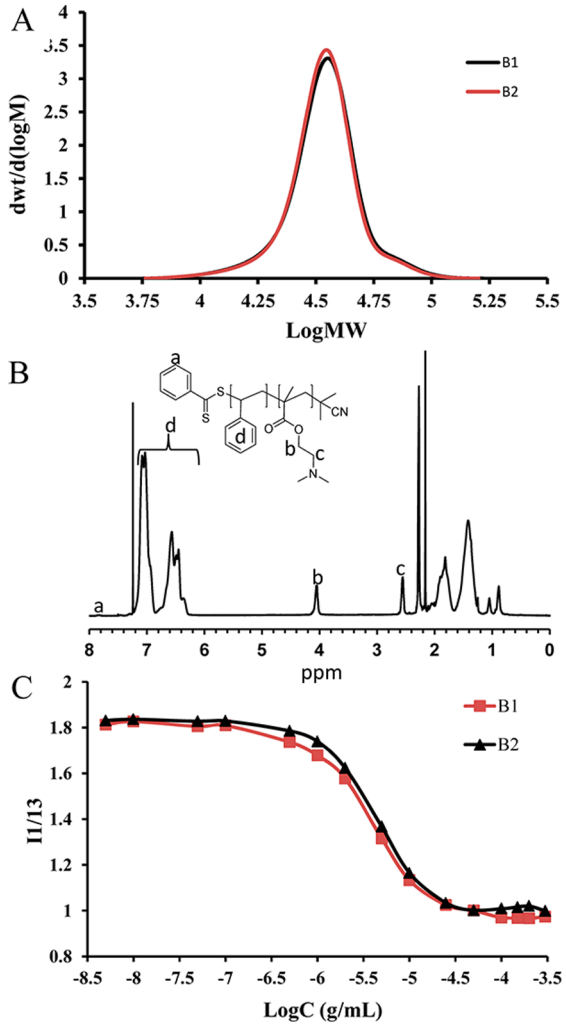

Figure 1. (A) Molecular weight distribution of B1 and B2 diblock copolymers, (B) ^{1}H NMR of B1 diblock copolymer in $CDCl_3$, and (C) I1/I3 fluorescence ratio of pyrene (I1 and I3 represent fluorescent intensity at 373 and 384 nm, respectively) in the presence of different concentrations of B1 and B2 diblock copolymers.

small, high molecular weight shoulder was observed in MWDs for B1 and B2 copolymer (see Figure 1A). This can be attributed to bimolecular termination stemming from the relatively high concentration of initiator used to increase the polymerization rate of styrene (i.e., 15 mol % to [macro-CTA]). That said, the PDI of these copolymers remained low (i.e., PDI = 1.14), which is very important for reproducibly yielding uniform morphologies. It has previously been demonstrated that a high PDI for a diblock copolymer impacts negatively on nearly every aspect of the self-assembly.[40] Data in Table 1 for two polymerization replicates (B1 and B2) showed very minor differences in molecular weight and number of repeat units, suggesting excellent reproducibility for the RAFT polymerizations under the conditions described here. Further, the critical micelle concentration (CMC) for B1 and B2 (determined by pyrene assay, see Figure 1C) was also very similar (∼1 μg mL^{-1}), which further confirmed the reproducibility of the polymer synthesis technique used herein.[41]

The well-defined P(DMAEMA-*b*-STY) diblock copolymer B1 and B2 were then used for the systematic self-assembly studies. Specifically, nanostructured aggregates with different morphologies (see Figure 2) were formed by the following procedure: the copolymer B1 (7.5 mg) was dissolved in an organic solvent (i.e., DMF, dioxane, or acetone), after which water was added (5 mL, addition rate 1.2 mL h^{-1}) to the organic solution to induce aggregation of the copolymer segments. Dialysis was then used to remove the organic solvent. The ratio of water to organic solvent in this study was kept constant at 10 to 1 to freeze the mobility of the PSTY cores and, thus, stabilize all formed morphologies at the end of the water addition.[42−44] DMF, dioxane, and acetone were chosen as organic solvents to give a representative range of solubility parameters (δ), and dielectric constants (ε), and to facilitate the formation of varying morphologies (i.e., spheres, vesicles, and worms, respectively).[24] Specifically, DMF, having a higher solubility parameter than that of PSTY (δ_{DMF} = 24.8 > δ_{PSTY} = 16.6−20.2) led to a lower amount of DMF being present in the PSTY core and a low aggregation number (N_{agg}) at the onset of micellization.[18] The low N_{agg} facilitates the formation of spherical morphology (see Figure 2A).[20] Dioxane (δ = 20.5) and acetone (δ = 19.7) each have a similar solubility parameter to that of PSTY and so can exhibit a higher N_{agg}, thus, resulting in the formation of bilayer morphologies (i.e., vesicles and worms).[45] Additionally, the ionizable P(DMAEMA) block was partially charged when water was added in a high dielectric constant solvent such as acetone (ε = 21.3), leading to a large effective volume of corona at the onset of micellization and the establishment of worm-like morphology.[46] By contrast, when water was added in a common solvent of lower dielectric constant like dioxane (ε = 2.2), the charge on the P(DMAEMA) block was negligible, and accordingly, the repulsion was weaker.[18] The reduced repulsion between polymer chains resulted in a smaller volume per corona chain on the micelle surface thereby facilitating the formation of vesicle morphology.[47] Further, Figure S3 shows that the morphologies formed using B2 are identical to those formed from B1 (see Figure 2) for all organic solvent choices. These results attest to the reproducibility of not only polymer synthesis, but also the self-assembly procedure. In short, by the judicious selection of organic solvents, nanoaggregates with three morphologies including SPH, VES, WLN were reproducibly obtained by the self-assembly of the P(DMAEMA$_{22}$-*b*-STY$_{215}$) diblock copolymer in water.

The effect of water addition rate and copolymer concentration on the formation of nanoaggregates was also examined. Figure 3 shows the different morphologies of nanoaggregates formed in water depending on the rates at which water was added to the acetone solution of B1. At faster addition rates, such as 5 mL s^{-1} and 24 mL h^{-1}, vesicle morphology was found. When the addition rate was reduced to 2.4 or 1.2 mL

DOI: 10.1021/acsmacrolett.5b00111
ACS Macro Lett. 2015, 4, 381−386

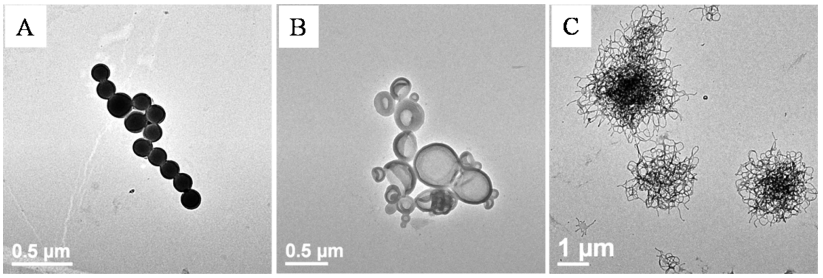

Figure 2. TEM images of the aggregates (A, SPH; B, VES; and C, WLN) formed by the self-assembly of B1 by adding water (5 mL, injection rate at 1.2 mL h^{-1}) to (A) DMF, (B) dioxane, and (C) acetone solutions of B1 (15 mg mL^{-1}). In each case, the volume of the organic solvent solution of B1 was 0.5 mL.

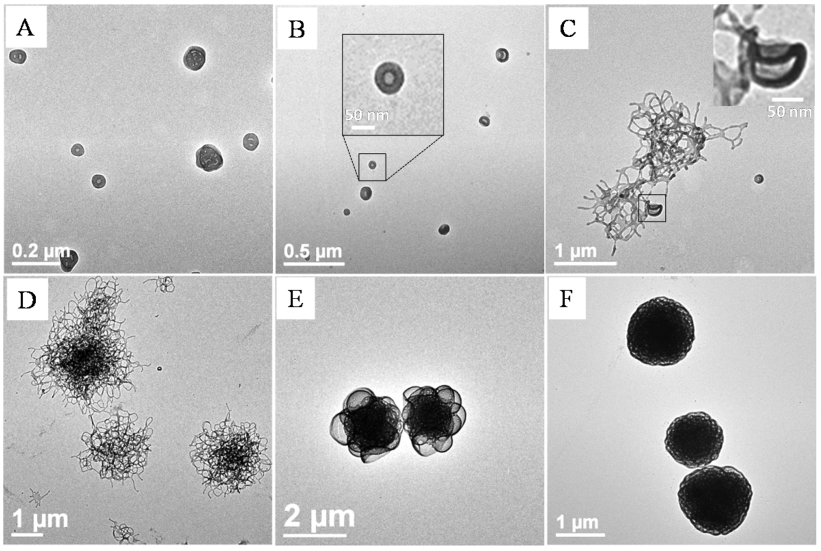

Figure 3. TEM images of the aggregates (A and B, VES; C and D, WLN; E, FLV; F, LCV) formed by self-assembly of B1 by adding water (5 mL) at different injection rates: (A) 5 mL s^{-1}, (B) 24 mL h^{-1}, (C) 2.4 mL h^{-1}, (D) 1.2 mL h^{-1}, (E) 0.4 mL h^{-1}, and (F) 0.1 mL h^{-1} to acetone solutions (0.5 mL) of B1 (15 mg mL^{-1}).

h^{-1}, worm-like morphology was mainly observed. Interestingly, when the addition rate was further decreased to either 0.4 or 0.1 mL h^{-1}, FLV and LCV were formed, respectively. The mixture of WLN and VES evident in Figure 3C suggested the possible transformation from vesicle to worm-like morphology when the addition rate was reduced from 24 to 2.4 mL h^{-1}. This vesicle-to-worm transition might be similar to the morphology transformation observed by Armes et al., when the block length of hydrophilic corona of poly(2-hydroxypropyl methacrylate) was decreased.[48] Additionally, Figure 3D−F possibly provide a trend in the transformation of WLN to FLV and finally to LCV. Taken together, these results suggest that VES, WLN, and FLV may be kinetically trapped morphologies formed at the fast water addition rates. On the other hand, the equilibrium morphology of LCV is able to form when water was added sufficiently slowly (i.e., over 50 h) to the B1 solution at the concentration of 15 mg mL^{-1} (see Figure 3F). At lower concentrations of B1 copolymer in acetone (5 and 10 mg mL^{-1}), the equilibrium morphology (i.e., LCV) could be obtained relatively faster (after about 13 and 130 min, respectively, see Figures S4 and S5). These observations may be attributed to the fact that, at room temperature and without plasticizer, the glassy PSTY cores are kinetically frozen (the glass transition temperature of PSTY is around 100 °C) resulting in the aggregate morphologies being effectively trapped.[49−51] Also in support of this morphology transformation is the fact that the solubility parameter of acetone (i.e., δ = 19.7) is very similar to that of PSTY (i.e., δ = 16.6−20.2). As such, the PSTY core can be swollen by acetone (which acts like a plasticizer) over a broad window of water content, thus, enabling morphology transformations through the increase of N_{agg}.[18] Therefore, a longer time of water addition, or with a lower concentration of copolymer in acetone, equilibrium morphology is attained. This explanation also accounts for why the addition rates do not affect the morphology of B1 copolymer in water when organic solvents with higher solubility parameters (such as DMF and dioxane were used, see Figures S6 and S7) were used. Altogether, by controlling the water addition rate and copolymer concentration, WLN, FLV, and LCV could be readily produced from the same B1 copolymer using this self-assembly technique.

The stability and reproducibility of the WLN, FLV, LCV, SPH, and VES, and the ability to incorporate fluorescent label into these nanoaggregates for biomedical studies were also investigated. To test the stability, each nanoaggregate was dialyzed against phosphate buffered saline for a week, after which the nanoaggregates were reimaged. TEM images in Figure S8 showed that all morphologies (including those which were kinetically trapped) were retained under these conditions. The stability of these morphologies is attributed to the aforementioned glassy PSTY cores. In addition, to facilitate the tracking and imaging of these materials in vitro and in vivo,

DOI: 10.1021/acsmacrolett.5b00111
ACS Macro Lett. 2015, 4, 381−386

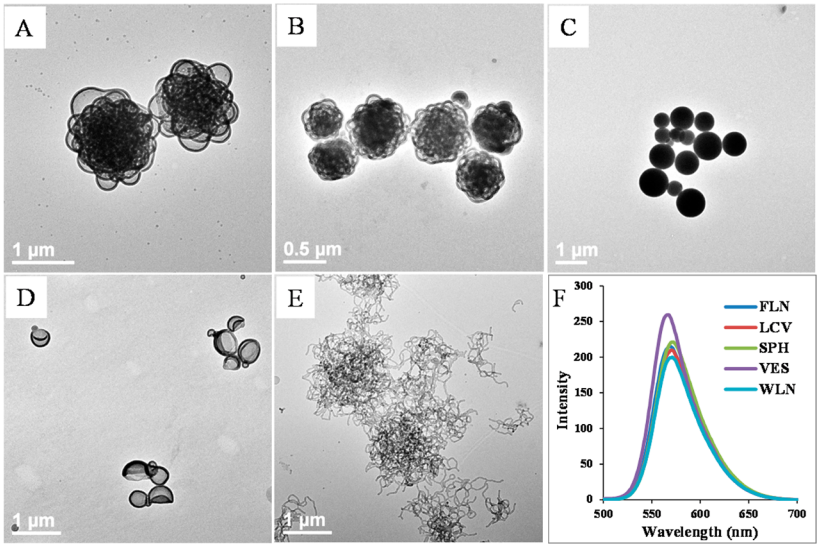

Figure 4. TEM images of the aggregates (A, FLV; B, LCV; C, SPH; D, VES; E, WLN) formed by self-assembly of (A) B2 and Nile red dye by adding water (0.4 mL h^{-1}) to a solution of B2 (15 mg mL^{-1}) and Nile red in acetone, (B) B2 and Nile red dye by adding water (1.2 mL h^{-1}) to a solution of B2 (0.2 mg mL^{-1}) and Nile red in acetone, (C) B2 and Nile red dye by adding water (1.2 mL h^{-1}) to a solution of B2 (5 mg mL^{-1}) and Nile red in DMF, (D) B2 and Nile red dye by adding water (1.2 mL h^{-1}) to a solution of B2 (15 mg mL^{-1}) and Nile red in dioxane, and (E) B2 and Nile red dye by adding water (1.2 mL h^{-1}) to a solution of B2 (15 mg mL^{-1}) and Nile red in acetone. (F) Fluorescence emission spectra of the aggregates with various morphologies formed using self-assembly condition as given in A–E. Nile red concentration in all samples was 20 μg mL^{-1}. In each case, volumes of organic solvent and added water were 0.5 and 5 mL, respectively.

labeling these nanoaggregates with fluorescent dye is necessary. Nile red was selected as a hydrophobic dye to coassemble with the P(DMAEMA-*b*-STY) diblock copolymer because of its strong fluorescent intensity in a hydrophobic environment (i.e., in the styrenic cores).[52] Moreover, Nile red fluorescence is completely quenched in water, which allows the dye location to be distinguished (i.e., between the hydrophobic nanoparticle cores and other domains such as the aqueous interior of a vesicle pocket).[52] Figure 4 shows five morphologies obtained from the self-assembly of B2 copolymer and Nile red in water (WLN, FLV, LCV, SPH, and VES), along with their fluorescence emission spectra. The same morphologies are observed when B1 copolymer is used (see Figure S8). In addition, fluorescent spectra of these nanoaggregates are also similar (see Figure 4F). These results confirm that it is possible to load a hydrophobic dye into the core of these nanoparticles without changing their morphology, and that the self-assembly procedures are reproducible. Further, Figure S9 shows that the WLN could be broken into short nanorods by applying ultrasound.[53,54] These short nanorods may be more useful for drug and gene delivery applications.[55] Finally, zeta potential data (see Table S2) confirm the expected positive charge of the nanoaggregates with various morphologies. Altogether, these results suggested that WLN, FLV, LCV, SPH, and VES could be reproducibly prepared, labeled by fluorescent dye, and were stable in buffer. Such particles are ideal for elucidating the importance of shape in drug and gene delivery.

In conclusion, a range of positively charged WLN, FLV, LCV, SPH, and VES were successfully prepared by manipulating the self-assembly conditions (i.e., organic solvent, water addition rate, and polymer concentration) for a single P(DMAEMA-*b*-STY) diblock copolymer in water. The preparation of these nanoaggregates was demonstrated to be both facile and reproducible. In each case, the morphology of the nanoparticles produced was uniform, stable in buffer, and the particles could be labeled by incorporating a hydrophobic fluorescent dye in the facile coassembly procedure. These novel positively charged nanoparticles, together with previously reported negatively charged and neutral nanoaggregates, provide a complete library of nanostructured particles with different morphologies and surface chemistry. This library will enable the fundamental study of the effect of morphologies and surface properties on interactions between nanoparticles with biological systems and will potentially provide novel nanocarriers for drug and gene delivery.

■ ASSOCIATED CONTENT

Supporting Information

Experimental procedures for preparation and characterization of all compounds, as well as TEM images and zeta potential details for all samples. This material is available free of charge via the Internet at http://pubs.acs.org.

■ AUTHOR INFORMATION

Corresponding Authors

*E-mail: michael.whittaker@monash.edu.
*E-mail: thomas.p.davis@monash.edu.

Notes

The authors declare no competing financial interest.

■ ACKNOWLEDGMENTS

This work was carried out within the Australian Research Council (ARC) Centre of Excellence in Convergent Bio-Nano Science and Technology (Project No. CE140100036). T.P.D. is grateful for the award of an Australian Laureate Fellowship from the ARC. N.P.T. acknowledges the financial support from Faculty of Pharmacy and Pharmaceutical Sciences, Monash University.

DOI: 10.1021/acsmacrolett.5b00111
ACS Macro Lett. 2015, 4, 381–386

REFERENCES

(1) Venkataraman, S.; Hedrick, J. L.; Ong, Z. Y.; Yang, C.; Ee, P. L. R.; Hammond, P. T.; Yang, Y. Y. *Adv. Drug Delivery Rev.* **2011**, *63*, 1228.
(2) Champion, J. A.; Katare, Y. K.; Mitragotri, S. *J. Controlled Release* **2007**, *121*, 3.
(3) Truong, N. P.; Whittaker, M. R.; Mak, C. W.; Davis, T. P. *Expert Opin. Drug Delivery* **2015**, *12*, 129.
(4) Brakhage, A. A.; Bruns, S.; Thywissen, A.; Zipfel, P. F.; Behnsen, J. *Curr. Opin. Microbiol.* **2010**, *13*, 409.
(5) Justice, S. S.; Hunstad, D. A.; Cegelski, L.; Hultgren, S. J. *Nat. Rev. Microbiol.* **2008**, *6*, 162.
(6) Geng, Y.; Dalhaimer, P.; Cai, S.; Tsai, R.; Tewari, M.; Minko, T.; Discher, D. E. *Nat. Nanotechnol.* **2007**, *2*, 249.
(7) Vivo, B.; Huang, X.; Li, L.; Liu, T.; Hao, N.; Liu, H.; Chen, D.; Tang, F. *ACS Nano* **2011**, *5*, 5390.
(8) Bruckman, M. A.; Randolph, L. N.; VanMeter, A.; Hern, S.; Shoffstall, A. J.; Taurog, R. E.; Steinmetz, N. F. *Virology* **2014**, *449*, 163.
(9) Karagoz, B.; Esser, L.; Duong, H. T.; Basuki, J. S.; Boyer, C.; Davis, T. P. *Polym. Chem.* **2014**, *5*, 350.
(10) Barua, S.; Mitragotri, S. *ACS Nano* **2013**, *7*, 9558.
(11) Shukla, S.; Wen, A. M.; Ayat, N. R.; Commandeur, U.; Gopalkrishnan, R.; Broome, A. M.; Lozada, K. W.; Keri, R. A.; Steinmetz, N. F. *Nanomedicine* **2014**, *9*, 221.
(12) Hu, X. L.; Hu, J. M.; Tian, J.; Ge, Z. S.; Zhang, G. Y.; Luo, K. F.; Liu, S. Y. *J. Am. Chem. Soc.* **2013**, *135*, 17617.
(13) Lee, E. S.; Oh, K. T.; Kim, D.; Youn, Y. S.; Bae, Y. H. *J. Controlled Release* **2007**, *123*, 19.
(14) Oh, K. T.; Oh, Y. T.; Oh, N. M.; Kim, K.; Lee, D. H.; Lee, E. S. *Int. J. Pharm.* **2009**, *375*, 163.
(15) Toy, R.; Peiris, P. M.; Ghaghada, K. B.; Karathanasis, E. *Nanomedicine* **2014**, *9*, 121.
(16) Caldorera-Moore, M.; Guimard, N.; Shi, L.; Roy, K. *Expert Opin. Drug Delivery* **2010**, *7*, 479.
(17) Daum, N.; Tscheka, C.; Neumeyer, A.; Schneider, M. *Wiley Interdiscip. Rev. Nanomed. Nanobiotechnol.* **2012**, *4*, 52.
(18) Mai, Y.; Eisenberg, A. *Chem. Soc. Rev.* **2012**, *41*, 5969.
(19) Quemener, D.; Deratani, A.; Lecommandoux, S. *Top. Curr. Chem.* **2012**, *322*, 165.
(20) Zhang, L. F.; Eisenberg, A. *Polym. Adv. Technol.* **1998**, *9*, 677.
(21) Rodriguez-Hernandez, J.; Checot, F.; Gnanou, Y.; Lecommandoux, S. *Prog. Polym. Sci.* **2005**, *30*, 691.
(22) Zhang, L. F.; Yu, K.; Eisenberg, A. *Science* **1996**, *272*, 1777.
(23) Zhang, L. F.; Eisenberg, A. *Science* **1995**, *268*, 1728.
(24) Cameron, N. S.; Corbierre, M. K.; Eisenberg, A. *Can. J. Chem.* **1999**, *77*, 1311.
(25) Wilson, J. T.; Keller, S.; Manganiello, M. J.; Cheng, C.; Lee, C. C.; Opara, C.; Convertine, A.; Stayton, P. S. *ACS Nano* **2013**, *7*, 3912.
(26) Liu, P. F.; Yu, H.; Sun, Y.; Zhu, M. J.; Duan, Y. R. *Biomaterials* **2012**, *33*, 4403.
(27) van de Wetering, P.; Zuidam, N. J.; van Steenbergen, M. J.; van der Houwen, O. A. G. J.; Underberg, W. J. M.; Hennink, W. E. *Macromolecules* **1998**, *31*, 8063.
(28) Sahnoun, M.; Charreyre, M. T.; Veron, L.; Delair, T.; D'Agosto, F. *J. Polym. Sci., Part A: Polym. Chem.* **2005**, *43*, 3551.
(29) Tan, B. H.; Gudipati, C. S.; Hussain, H.; He, C. B.; Liu, Y.; Davis, T. P. *Macromol. Rapid Commun.* **2009**, *30*, 1002.
(30) Truong, N. P.; Jia, Z.; Burges, M.; McMillan, N. A.; Monteiro, M. J. *Biomacromolecules* **2011**, *12*, 1876.
(31) Tran, N. T. D.; Truong, N. P.; Gu, W. Y.; Jia, Z. F.; Cooper, M. A.; Monteiro, M. J. *Biomacromolecules* **2013**, *14*, 495.
(32) Zhang, L. F.; Eisenberg, A. *Macromolecules* **1996**, *29*, 8805.
(33) Gu, W. Y.; Jia, Z. F.; Truong, N. P.; Prasadam, I.; Xiao, Y.; Monteiro, M. J. *Biomacromolecules* **2013**, *14*, 3386.
(34) Hartono, S. B.; Phuoc, N. T.; Yu, M. H.; Jia, Z. F.; Monteiro, M. J.; Qiao, S. H.; Yu, C. Z. *J. Mater. Chem. B* **2014**, *2*, 718.
(35) Kolhar, P.; Anselmo, A. C.; Gupta, V.; Pant, K.; Prabhakarpandian, B.; Ruoslahti, E.; Mitragotri, S. *Proc. Natl. Acad. Sci. U.S.A.* **2013**, *110*, 10753.
(36) Kolhar, P.; Doshi, N.; Mitragotri, S. *Small* **2011**, *7*, 2094.
(37) Barua, S.; Yoo, J. W.; Kolhar, P.; Wakankar, A.; Gokarn, Y. R.; Mitragotri, S. *Proc. Natl. Acad. Sci. U.S.A.* **2013**, *110*, 3270.
(38) Zhang, L. F.; Eisenberg, A. *J. Am. Chem. Soc.* **1996**, *118*, 3168.
(39) Yu, Y. S.; Zhang, L. F.; Eisenberg, A. *Macromolecules* **1998**, *31*, 1144.
(40) Lynd, N. A.; Meuler, A. J.; Hillmyer, M. A. *Prog. Polym. Sci.* **2008**, *33*, 875.
(41) Chen, W.; Zhong, P.; Meng, F. H.; Cheng, R.; Deng, C.; Feijen, J.; Zhong, Z. Y. *J. Controlled Release* **2013**, *169*, 171.
(42) Discher, D. E.; Eisenberg, A. *Science* **2002**, *297*, 967.
(43) Battaglia, G.; Ryan, A. J. *Macromolecules* **2006**, *39*, 798.
(44) Shen, H. W.; Zhang, L. F.; Eisenberg, A. *J. Am. Chem. Soc.* **1999**, *121*, 2728.
(45) Barton, A. F. M. *CRC Handbook of Solubility Parameters and Other Cohesion Parameters*; 2nd ed.; CRC Press: Boca Raton, FL, 1991.
(46) Mohsen-Nia, M.; Amiri, H.; Jazi, B. *J. Solution Chem.* **2010**, *39*, 701.
(47) Israelachvili, J. N. *Intermolecular and Surface Forces*, 3rd ed.; Academic Press: Waltham, MA, 2011; p 1.
(48) Blanazs, A.; Madsen, J.; Battaglia, G.; Ryan, A. J.; Armes, S. P. *J. Am. Chem. Soc.* **2011**, *133*, 16581.
(49) Jia, Z. F.; Truong, N. P.; Monteiro, M. J. *Polym. Chem.* **2013**, *4*, 233.
(50) Gan, Y. D.; Dong, D. H.; Hogenesch, T. E. *Macromolecules* **1995**, *28*, 383.
(51) Kessel, S.; Truong, N. P.; Jia, Z. F.; Monteiro, M. J. *J. Polym. Sci., Part A: Polym. Chem.* **2012**, *50*, 4879.
(52) Castro, G. R.; Larson, B. K.; Panilaitis, B.; Kaplan, D. L. *Appl. Microbiol. Biotechnol.* **2005**, *67*, 767.
(53) Jia, Z. F.; Bobrin, V. A.; Truong, N. P.; Gillard, M.; Monteiro, M. J. *J. Am. Chem. Soc.* **2014**, *136*, 5824.
(54) Wang, X.; Guerin, G.; Wang, H.; Wang, Y.; Manners, I.; Winnik, M. A. *Science* **2007**, *317*, 644.
(55) Barua, S.; Mitragotri, S. *ACS Nano* **2013**, *7*, 9558.

DOI: 10.1021/acsmacrolett.5b00111
ACS Macro Lett. 2015, 4, 381−386